

Double spiral steps on Ih ice crystal surfaces grown from water vapor just below the melting point

*Gen Sazaki**, Harutoshi Asakawa, Ken Nagashima, Shunichi Nakatsubo, Yoshinori Furukawa
Institute of Low Temperature Science, Hokkaido University, N19-W8, Kita-ku,
Sapporo 060-0819, Japan

Contents

Fig. S1. Schematic drawings of the experimental setups.

Fig. S2. Image processing performed to obtain the LCM-DIM images shown in this paper.

Fig. S3. Differential interference contrast adopted in this paper.

Video S1. Time course of the coalescence of spiral steps and 2D island steps on an ice basal face at -3.0°C (Fig. 2).

Other Supporting Online Material for this manuscript includes Video S1.

* To whom correspondence should be addressed. E-mail: sazaki@lowtem.hokudai.ac.jp

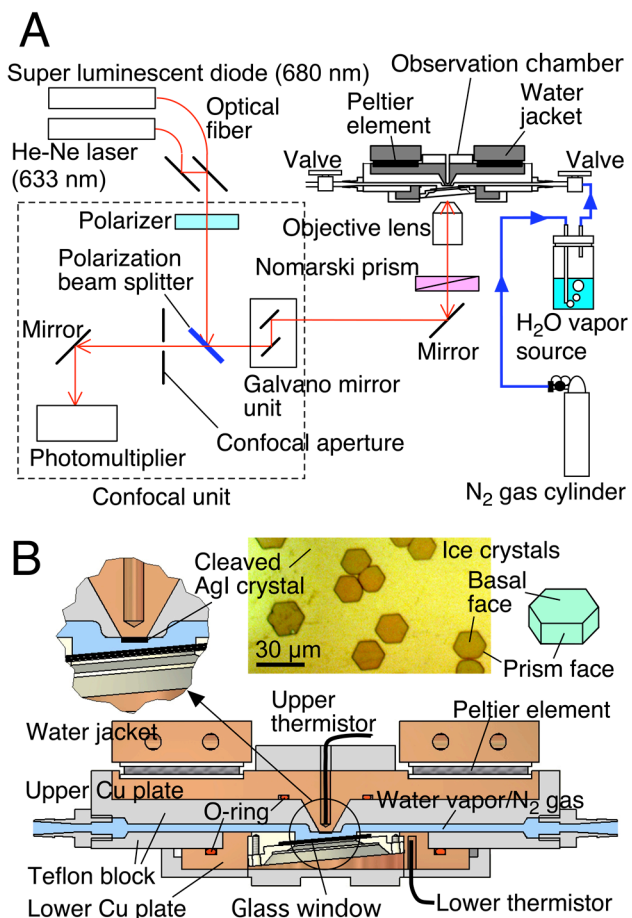


Fig. S1. Schematic drawings of the experimental setups (This figure was reprinted from Fig. S2 of ref.²). (A) The LCM-DIM system, the observation chamber and the water-vapor supply system, (B) a cross-sectional view of the observation chamber. In B, the upper left inset shows a closeup view of the cleaved AgI crystal attached to the upper Cu plate using heat grease, the upper center inset presents a photomicrograph of Ih ice crystals grown heteroepitaxially on the AgI crystal, and the upper right inset depicts the morphology of the Ih ice crystal. The surface of the cleaved AgI crystal was observed from below through a glass window that was tilted to prevent the appearance of interference fringes.

We grew Ih ice single crystals on a cleaved {0001} face of the AgI crystal from supersaturated water vapor in a nitrogen environment. We set the temperature of the ice single crystals to -15.0°C . To supply water vapor to the sample ice crystals, we prepared other ice crystals (as a source of water vapor) on the lower copper plate. By separately changing the temperatures of the upper and lower Cu plates, we adjusted the growth temperature of the sample ice crystals and the supersaturation of the water vapor independently.

Sample ice crystals on the cleaved AgI crystal were ≥ 16 mm distant from the source ice crystals prepared on the lower Cu plate. The temperature of the teflon block was not controlled. Therefore, as water vapor diffused away from the source ice crystals in N_2 gas at atmospheric pressure, its temperature increased. Hence, the temperature of the water vapor in the vicinity of the sample ice crystals was unclear. Therefore, in our observations, the degree of supersaturation could not be quantified. However, throughout the experiment, we kept the sample ice crystals growing by carefully changing the temperature of the source ice crystals and confirming the growth by LCM-DIM observation.

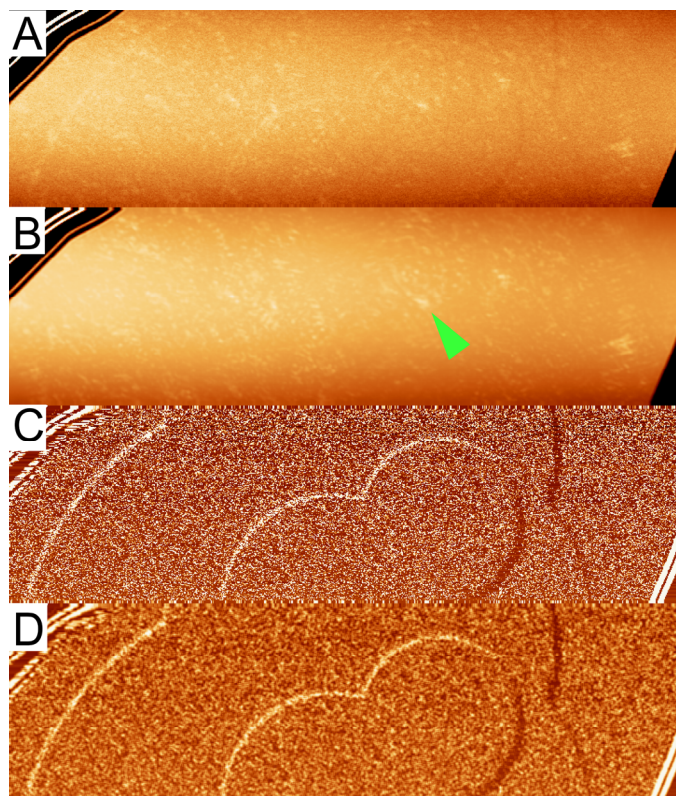


Fig. S2. Image processing performed to obtain the LCM-DIM images shown in this paper (This figure was reprinted from Fig. S1 of ref.¹). A time-averaged image (B) was subtracted from the original image (A). In B, motionless objects such as defects (marked by a green arrowhead) and the inhomogeneous background level were extracted. After the gain and offset of the subtracted image had been adjusted (C), a Gaussian filter that was one pixel in size was used (D) to smooth the image.

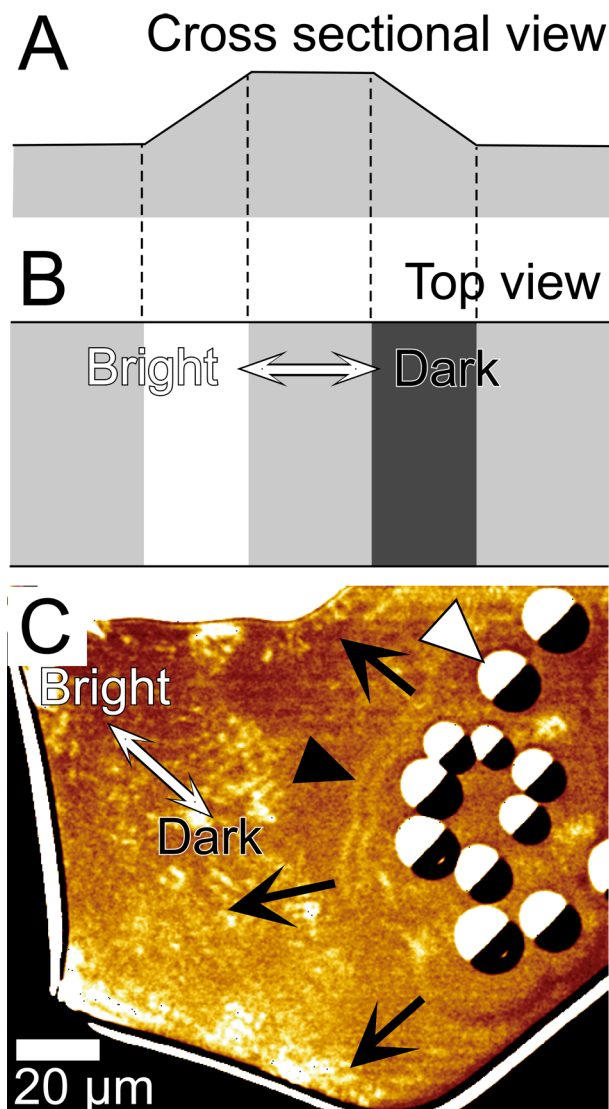


Fig. S3. Differential interference contrast (This figure was reprinted from Fig. S5 of ref.²). Utilizing interference of polarized light, differential interference contrast microscopy provides a contrast level so that the slopes of one side and the other side of a convex object look brighter and darker (white arrow), respectively, as schematically shown in A and B (as if a sample surface is illuminated from one slanted direction). Hence, in all LCM-DIM images shown in this paper, the upper left sides of the drops and steps appear brighter and the lower right sides of them appear darker (white arrow), as shown in C. In C, other arrows and arrowheads are the same as those in Fig. 1.

Video S1. Time course of the coalescences of spiral steps and 2D island steps on an ice basal face at -3.0°C . A part of this video is shown as Fig. 2. To obtain these images, raw images were processed according to the recipe explained in Fig. S2. The frame rate was 0.70 s/frame. To reduce the file size, the video file was converted from 816x236 pixels to 408x118 pixels.